Cement and Concrete Research 189 (2025) 107766

Contents lists available at ScienceDirect

Cement and Concrete Research

journal homepage: www.elsevier.com/locate/cemconres

Reaction kinetics of calcined smectite in a clinker-free model and a synthetic cement system in comparison with selected calcined phyllosilicates

Sebastian Scherb [a,*], Matthias Maier [b], Köberl Mathias [a], Nancy Beuntner [a], Karl-Christian Thienel [a]

[a] Civil Engineering and Environmental Science, University of the Bundeswehr Munich, Werner-Heisenberg-Weg 39, 85579 Neubiberg, Germany
[b] Group for Sustainable Binders, Fraunhofer IBP, Fraunhoferstr. 10, 83626 Valley, Germany

ARTICLE INFO

Keywords:
Calcined clay
Smectite
Supplementary cementitious material
Reaction kinetics
Calorimetry
In situ X-ray diffraction

ABSTRACT

The investigations of clinker-free model and synthetic cement systems reveal deeper insight into the behavior of metasmectite during early hydration. The use of metasmectite accelerates the aluminate clinker reaction and influences the degree of hydration of alite. Its chemical reactivity can be demonstrated in clinker-free as well as model cement systems by direct quantification of the metasmectite, its portlandite consumption and C-S-H formation. The influence on sulfate balance reveals an interaction of metasmectite's negatively charged surfaces with ions from the pore solution and demonstrates that sulfate adsorption does not solely take place on surfaces of C-S-H. Overall, it can be concluded that the impediment of the alite hydration during early hydration due to metasmectite is rather insignificant compared to metakaolinite and is within the range of metaillite. These findings provide a significant contribution to the expected widespread use of calcined clays with a low metakaolinite content in cementitious systems.

1. Introduction

The widespread use of calcined clays (CC) will depend crucially on the utilization of different clay sources, including a variation of the amount of 1:1 and 2:1 clay minerals. This is indispensable, as the demand for concrete and thus for clinker-reduced binders will further rise [1]. Therefore, understanding the influence of calcined clays during early hydration of blended cement is essential for their widespread use in modern cements and concretes. Common clays are a mixture of different phyllosilicates and accompanying minerals and thus represent a very complex material with divergent mineralogical composition, chemical reactivity and surface properties [2,3]. This complexity is reflected in the influence of CC on the silicate and aluminate clinker reaction during early hydration, which is still the subject of current discussions. The surface properties and thus the adsorption of ions from the pore solution on the surfaces of the C_3A [4], the surfaces of the C-S-H [5,6], as well as directly on the surfaces of the CC [7–10], and the reactivity of the CC itself at very early stages of cement hydration [8,10,11] have been identified in various studies as key parameters for influencing the sulfate balance. Even if there is a correlation between the formation of C-S-H (alite reaction) and the dissolution of the sulfate carriers for pure cement systems [6,12,13], studies have shown that this cannot be the only factor when CC is used [9,10]. Accordingly, the surfaces of the C-S-H are not sufficient to adsorb the sulfate completely and additional surfaces are required. Furthermore, the reactivity of the CC influences the sulfation of the systems, as investigations on clays with a high metakaolinite (MK) or metaillite (MI) content confirmed [7,10].

Calcined Smectite (metasmectite, MS) has been identified as the most reactive 2:1 clay mineral in cementitious systems [14–16]. Therefore smectite-rich clays have attained increased attention as a promising extension to kaolinitic clays [17]. However, the impact of MS on the early hydration of blended cements has not been addressed so far, apart from the well-known fact, that MS reacts significantly slower compared to MK with regards to portlandite consumption [16,17]. The dissolution of MS in alkaline systems is approx. one fourth compared to MK and appears to be an incongruent process [18]. Werling et al. [19] found that this incongruent dissolution behavior of MS is more pronounced during the early dissolution phase (<24 h) than after 7 d. MI, on the other hand,

* Corresponding author.
E-mail addresses: sebastian.scherb@unibw.de (S. Scherb), matthias.maier@ibp.fraunhofer.de (M. Maier), mathias.koeberl@unibw.de (K. Mathias), nancy.beuntner@unibw.de (N. Beuntner), christian.thienel@unibw.de (K.-C. Thienel).

https://doi.org/10.1016/j.cemconres.2024.107766
Received 22 July 2024; Received in revised form 28 November 2024; Accepted 4 December 2024
Available online 8 December 2024

shows congruent dissolution behavior for moderate calcination temperatures in the range between 650 and 800 °C [19,20].

The present study focuses primarily on MS and belongs to a series of preceding systematic investigations of MK, MI and metamuscovite (MM) [8,10]. Both, in clinker-free model systems and in model cement systems, in situ XRD quantification of the early reactions during the first 50 h provides a deeper insight into the behavior of MS. The comparison of the 1:1 calcined phyllosilicate (meta-phyllosilicate) MK and various 2:1 meta-phyllosilicates (MS, MI and MM) contributes significantly to the knowledge of complex composite cements with the addition of CC.

2. Materials and methods

2.1. Characterization of metasmectite

The examined smectite is a montmorillonite dominated clay from the Westerwald region (Germany). The characterization of metasmectite (MS) is based on the characterization of the meta-phyllosilicates metakaolinite (MK), metaillite (MI) and metamuscovite (MM) in [8,10]. The smectite was calcined in platinum crucibles at 800 °C for 30 min in a preheated muffle furnace. After calcination, the sample was cooled in a desiccator at room temperature. The calcination temperature was chosen based on the dehydroxylation peak of thermogravimetric analysis. A detailed description of the methods used for characterization can be found in publications of clinker-free model systems [8,21]. Table 1 summarizes the physical parameters as well as the zeta potential of the metasmectite investigated in a synthetic model pore solution according to [22]. Table 2 provides its chemical and mineralogical composition.

2.2. Clinker-free model systems

The investigations on the clinker-free model systems with MS were carried out in alkaline solution (100 mmol l^{-1} sodium hydroxide (NaOH) and 500 mmol l^{-1} potassium hydroxide (KOH)) with a liquid to solid ratio of 1.0 and portlandite (CH) as reaction partner. Two test series were carried out with and without sulfate carrier (C$). The nomenclature of the systems is based on their components MS-CH (50 wt-% MS and 50 wt-% CH without sulfate) and MS-CH-C$ (45 wt-% MS, 45 wt-% CH and 10 wt-% calcium sulfate (C$)).

2.3. Synthetic cement (SyCEM) systems

The synthetic cement (SyCEM) consists of the magnesium and aluminum stabilized M3 polymorph of alite and cubic tricalcium aluminate (C_3A). Gypsum and bassanite were used as sulfate carrier. A second reference system was prepared with 10 wt.-% of limestone powder (SyCEM-10LL). The procedure for clinker synthesis and the specifications of the limestone powder are given in [10]. The composition of the reference systems and their specific surface areas (Blaine) are provided in Table 3. The composition of the reference systems was chosen so that the silicate and aluminate peaks could be observed separately in the calorimeter, thus enabling a better assessment of the influence of the meta-phyllosilicates on the respective reactions.

The two reference systems were each substituted with 20 wt-%. of metasmectite. The designation of the resulting systems corresponds to their compositions (SyCEM-20MS or SyCEM-10LL-20MS). The w/b value for all tests is 0.6 in order to achieve proper homogenization and preparation despite the high water demand of the meta-phyllosilicates.

Table 1
Specific surface area (BET), particle density (PD), particle size distribution (PSD) and zeta potential of the metasmectite.

	MS
BET [m^2/g] [23]	37.9
PD [$g\ cm^{-3}$] [24]	2.71
d_{10} [μm]	5.2
d_{50} [μm]	21.8
d_{90} [μm]	7.4
Zeta potential [mV]	−9.0

Table 2
Chemical and mineralogical composition of the metasmectite.

Oxides (wt.-%)	MS	Phases (wt.-%)	MS
SiO_2	59.5	Smectite[a]	27
Al_2O_3	19.3	Illite/Mica	4
Fe_2O_3	9.0	Quartz	15
CaO	2.9	Feldspar	11
MgO	1.9	Anatase	2
SO_3	<0.1		
Na_2O	1.1		
K_2O	1.4		
TiO_2	2.1		
LOI	1.3	X-ray amorphous	39

[a] The smectite content of the raw clay is 60 ± 3 wt.-%.

Table 3
Composition of the two reference systems in [wt-%] and their specific surface area (Blaine) in [m^2/g].

	Alite	C_3A_{cubic}	Gypsum	Bassanite	LL	Blaine
SyCEM	87.25	8.5	3.5	0.75	–	≈4050
SyCEM-10LL	78.525	7.65	3.15	0.675	10	≈4100

2.4. Test program

This section describes briefly the various tests conducted within this investigation. Further details regarding the experimental setup are given in [8,10,25]. Thermogravimetry, isothermal calorimetry and in situ X-ray diffraction were performed for clinker-free model systems as well as for the model cement systems. The materials were equilibrated overnight in a heating cabinet at measurement temperature (25 °C), stirred manually with a spatula for 60 s directly before the start of the measurements and then immediately transferred to an appropriate crucible. The measurement temperature of 25 °C allows synchronizing the clinker-free and cementitious systems on the one hand, and the calorimetry and in situ XRD tests on the other, without significant unintentional desiccation of the Kapton film covered sample during the in situ XRD measurement. In addition, the solubilities of silicon and aluminum were determined time-dependently after 6 h, 20 h, 48 h and 7 d in the alkaline solution used for the clinker-free model systems (Section 2.2) according to Buchwald and Kaps [26]. The values after 7 d supplement the already published data of the MK, MI and MM [8]. The reactivity test (R^3) of the meta-phyllosilicates was performed by isothermal calorimetry according to ASTM C1897–20 [27].

Thermogravimetric (TG) investigations were carried out with Netzsch STA 449 F3. The exact process for sample preparation and the experimental procedure and formulas used for calculating the bound water and CH content is explained in [8,25]. The bound water was determined using the temperature interval from 20 to 400 °C and the CH content in the temperature interval between 450 and 550 °C.

Isothermal calorimetry experiments were performed with TA instruments TAM Air calorimeter at 25 °C for 50 h with 2 g of quartz sand in the reference chamber. The heat flow was normalized to 1 g of solid in case of clinker-free model systems [8] and to 1 g of the SyCEM in case of the synthetic cement systems [10].

In situ XRD measurements were conducted with a PANalytical Empyrean diffractometer equipped with a primary Bragg–BrentanoHD monochromator and a PIXcel^{1D} linear detector. The experimental setup is given in [8,10]. The measurements were quantified using Rietveld refinement [28,29] with a combination of G-factor and PONKCS method [30,31] according to Bergold et al. [32] with High Score 4.8 [33].

Table 4
Phases, authors and ICSD numbers used for Rietveld refinement.

Phase	Author	ICSD-No.
Silicon	[34]	52266
Alite	[35]	94742
C_3A_{cubic}	[36]	1841
Gypsum	[37]	92567
Anhydrite	[38]	16382
Smectite	[39]	161171
Illite	[40]	166963
Muscovite	[41]	68548
Quartz	[42]	174
Anatase	[43]	9852
Anorthite	[44]	22022
CH	[45]	34241
AFt	[46]	155395
AFm-Hc[a]	[47]	263124
Tobermorite[b]	[48]	403090
Kuzelite[c]	[49]	100138

[a] Hemicarboaluminatehydrate.
[b] Structure information used for creating hkl-phase model for C-S-H.
[c] Structure information used to quantify Calcium Aluminum Sulfate Hydrate ($Ca_4Al_2O_6(SO_4)$ × 14 H_2O PDF-Nr: 42-0062 [50], abbreviation:$C_4A\$$ × H_{14}, monosulfate).

Table 4 lists all structures used for Rietveld refinement. For the application of the PONKCS method, hkl phase models were developed (Kapton film) and calibrated as explained in [8,10,25]. The same procedure was applied to create and calibrate the hkl-phase model of MS. A schematic illustration of the refinement routine is given in [8]. For MS, both the scaling factor of the hkl-phase models and the crystalline structure were refined and presented as a sum.

The evaluations of the degree of hydration (DoH) of alite, the degree of reaction (DoR) of MS, the calculation of CH consumption and C-S-H formation as well as the key data concerning the aluminate reaction were carried out in the same way as for MK, MI and MM as described elsewhere [10]. For a better comparison and classification of the results of the MS, data from [10] is also shown in the graphs of the evaluations in the present work.

3. Results and discussion

3.1. Reactivity of metasmectite

The time-dependent solubility of silicon and aluminum in alkaline solution (see Section 2.2) after 6 h, 20 h, 48 h and 7 d of the meta-phyllosilicates is shown in Fig. 1. Up to 48 h the results of the ion solubility are in the order MK > MI > MS > MM. After 7 d, MS yields a higher solubility compared to MI and thus has a higher increase between 48 h and 7 d which holds as well in comparison to MK. This observation correlates very well with the development of the heat evolution of the meta-phyllosilicates in the reaction test (Fig. 2). While MS still exhibits a significant increase in heat of reaction beyond 48 h, MK and MI have almost completed their heat development at 48 h and reveal no further significant reaction. Thereby, it must be mentioned that the meta-phyllosilicate content is lower in the case of MS than the other meta-phyllosilicates. The ion solubility as well as the heat of hydration is low for MM in both cases over the entire test period of 7 d.

The time dependent correlation of the evolved heat and ion solubility (Fig. 3) yields to a very good regression (R^2 = 0.99) over all 16 data points (four meta-phyllosilicates at four different points in time, see Fig. 1). This confirms that, in addition to the heat of reaction, the solubility of Si and Al can be used as a parameter for the reactivity of CC regardless of the type of meta-phyllosilicate. However, a distinct comparison of the 2:1 meta-phyllosilicates MS and MI shows a slight differentiation. While the values of MS tend to be above the regression line (black dashed line in Fig. 3), the values of MI are below the regression line. As described for metasmectite by Garg and Skibsted [18] and Werling et al. [19], an incongruent dissolution of Si and Al for MS compared to MI might explain the observed differences and serve as a driving force, which leads to a higher reactivity of MS than of MI after two days onwards.

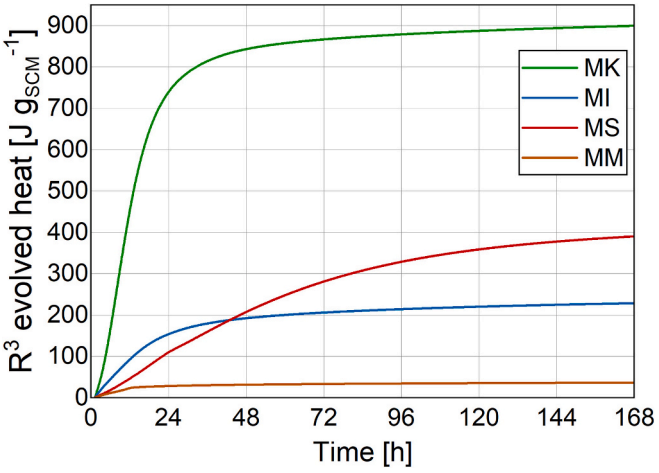

Fig. 2. Reactivity test (R^3) by isothermal calorimetry according to ASTM C1897-20 [27].

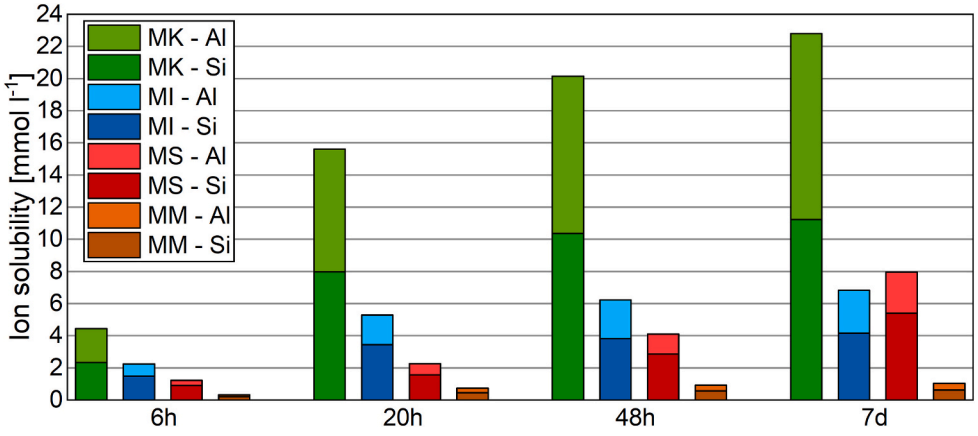

Fig. 1. Time-dependent silicon (Si) and aluminum (Al) solubility in alkaline solution after 6, 20, 48 h and 7 d.

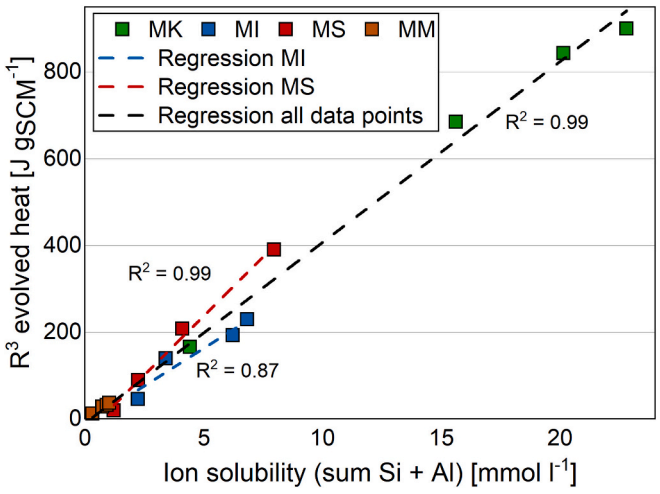

Fig. 3. Time dependent correlation of the R^3 evolved heat and ion solubility (sum of Si and Al) at 6, 20, 48 h and 7 d of MS in comparison with MK and MI.

3.2. Investigations of the clinker-fee model systems

Fig. 4 shows the results of the TG analyses. CH is already consumed by the pozzolanic reaction during the first 6 h both with and without sulfate. Nevertheless, the amount of water bound (H_{bound}) in the hydrate phases formed (products of the pozzolanic reaction) are low at this point in time. After 48 h, differences between the two systems are more clearly recognizable and the system with sulfate has a higher CH consumption and more bound water. This is mainly due to the formation of AFt in the presence of sulfate.

The results of the in situ XRD investigations and calorimeter measurements of the clinker-free model systems are combined in Fig. 5. Error bars of a duplicate determination were added for the corresponding phases after 50 h. At the beginning (during the first 4–5 h), an initial, accelerated dissolution of the CH can be observed. No crystalline hydrate phases can be quantified at this point. The bound water

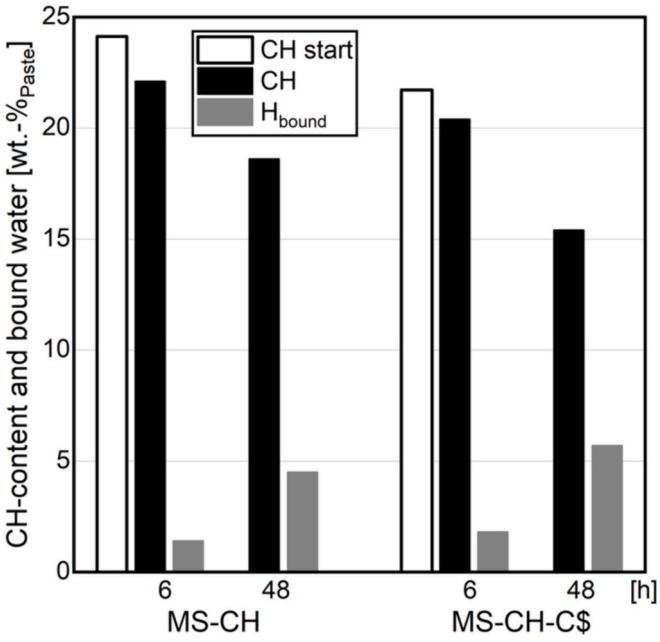

Fig. 4. Results of the TG investigations (CH-content and bound water) of the clinker-free model systems without sulfate (MS-CH, left side of the graph) and with sulfate (MS-CH-C$, right side of the graph) after 6 and 48 h. CH start is the starting point after mixing the powder sample with water.

determined by the TG measurements can be explained by poorly crystalline C-S-H phases at early ages according to Bergold et al. [32]. Thereafter the CH dissolution continues on a lower level until the end of the measurement. A similar observation can be made for the dissolution behavior of MS. The quantifications show a continuous dissolution process and no interval with a significant reaction as can be observed for MK [8]. A first C-S-H ("long-range-ordered" [32]) formation can be quantified approx. 35 h after water addition. The addition of C$ (Fig. 5, right graph) leads to AFt formation after approx. 18 h, which progresses steadily until the end of the measurement. The heat flow measurements also reflect the XRD quantifications of the MS systems. Following the initial heat flow, the system with sulfate (MS-CH-C$) yields a higher heat flow over the entire measurement period with a slight maximum at the beginning of AFt formation. Overall, MS exhibits a similar reaction behavior as MI during the first two days in the clinker-free model systems [8]. The high amount of dissolved CH and C$ in comparison to hydrate phases formed indicates adsorption of calcium and sulfate on the surface of MS particles as described by Maier et al. for kaolinitic and illitic clay surfaces [7] and by Myers et al. [4] for C_3A surfaces.

3.3. Investigations of the model cement systems

The results of the TG investigations after 6 and 48 h of the model cement systems are provided in Fig. 6. The differences are very small after 6 h both for the CH content and in the bound water up to 400 °C. In contrast, after 48 h there are clearer differences visible between references and systems containing MS, especially concerning the CH content. This indicates CH consumption by the pozzolanic reaction of the MS. Differences in the DoH of the alite can be assumed as a further explanation for the lower CH content compared to the references.

The results of the in situ XRD investigations and calorimeter measurements of the model cement systems containing MS are combined in Fig. 7. Error bars of a duplicate determination were added for the corresponding phases after 50 h. Additionally, the calorimeter curve of the reference systems from [10] is provided. The calorimeter measurements indicate a slight acceleration of the silicate reaction and a pronounced acceleration of the aluminate reaction due to the addition of MS. The results are in line with the observations obtained with MK, MI and MM [10]. This also applies for the in situ XRD quantifications which reveal an initial aluminate reaction through C_3A and sulfate carrier dissolution, as well as AFt formation after the first scan (15 min). As already shown by Hesse [51], complete sulfate carrier dissolution is accompanied by accelerated AFt formation until the maximum AFt content (AFt_{max}) is reached. The formation of monosulfate at the expense of AFt can be observed in the subsequent progress of the reaction in the LL-free system. The addition of LL promotes the formation of hemicarboaluminate hydrate, as predicted by thermodynamic modeling [52,53]. The silicate clinker reaction starts with a clear dissolution of alite and the formation of CH at the end of the dormant period. The first C-S-H can be observed at a later time (delay of 2–3 h), which is associated with the later formation of quantifiable "long-range-ordered" C-S-H according to Bergold et al. [32]. This is in line with the clinker-free model systems described in Section 3.2.

3.4. Evaluation and discussion of the results

3.4.1. Implications regarding the reactivity of meta-phyllosilicates

Fig. 8 summarizes the DoR of the four meta-phyllosilicates of the clinker-free model systems (a) and the model cement systems (a) derived from in situ XRD quantifications. The values of MK, MI, and MM are taken from [8,10]. Despite the clear error propagation when calculating the DoR from XRD quantifications, which have been discussed in detail [54,55], clear trends are visible and can be identified. Adding sulfate to the clinker-free model systems leads to a higher DoR for MS, as observed before for other meta-phyllosilicates. This can be attributed to sulfate as reaction partner for the aluminum of the meta-phyllosilicates and is

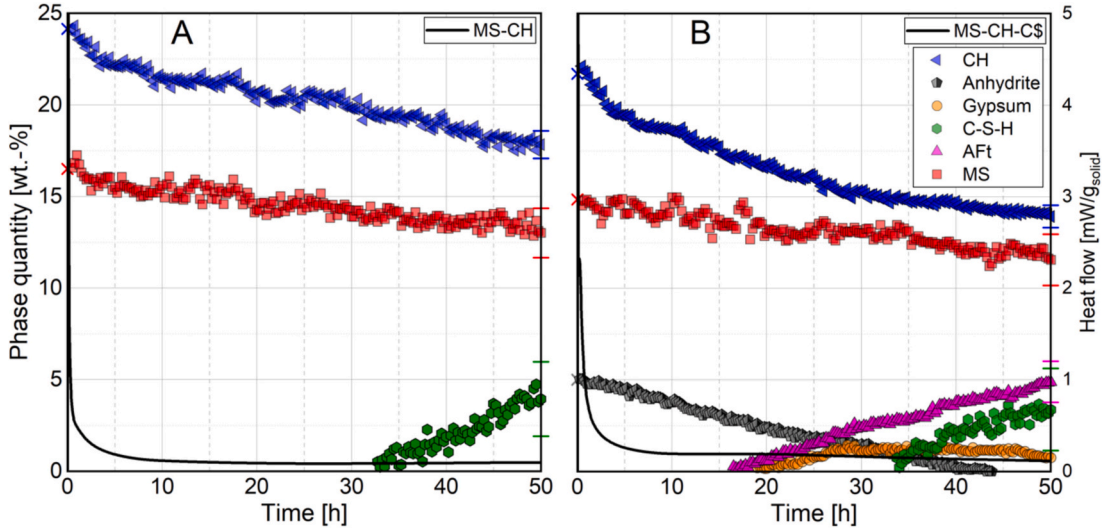

Fig. 5. Combined illustration of in situ XRD quantifications (left y-axis) and calorimeter measurements (right y-axis) of the clinker-free model systems of MS without sulfate (A) and with sulfate carrier (B). The error bar of a duplicate determination after 50 h is shown. In the case of MS, this was used to calculate its degree of reaction.

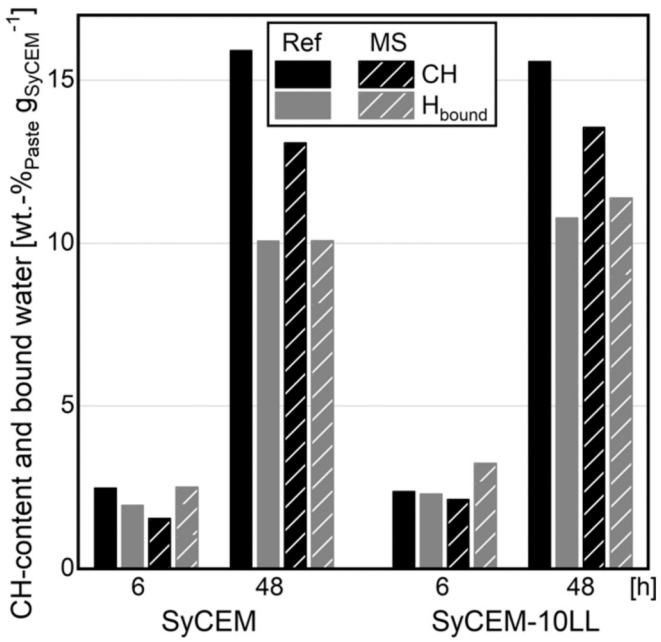

Fig. 6. Results of the TG investigations (CH-content and bound water) of the model cement system (SyCEM, left side of the graph) and the cement system with LL (SyCEM-10LL, right side of the graph) after 6 and 48 h. The values of the reference systems are taken from [10].

therefore caused by the AFt formation. The significantly higher DoR of MK supports this hypothesis, since MK provides by far the most aluminum for the reaction. Without the formation of calcium aluminate hydrates in the absence of sulfate, the high aluminum content might lead to an increased concentration of aluminum in the pore solution, which hinders further dissolution of the meta-phyllosilicates. The incorporation of aluminum into the C-S-H phases does not appear to be sufficient. The DoR of the meta-phyllosilicates in the model cement systems differs less. It is noticeable that the degree of reaction of the MK with LL (SyCEM-10LL) decreases in comparison to the model cement (SyCEM). For MI and MS, the tendency is the other way around, whereby the differences between the model cements are rather small and thus within the error of quantification with the PONKCS method [56]. MM has a very low reactivity in all systems (clinker-free and model cement) and can be regarded as a filler rather than a reactive SCM, as already reported [10]. This confirms the results of the R^3 test and is in line with the classification of inert material according to Snellings [57] with an evolved heat of <100 J/g SCM. Overall, the quantifications show comparable DoR for MS and MI after the first two days.

The DoR derived by XRD quantifications of the meta-phyllosilicates is correlated with the evolved heat of the reaction test in Fig. 2 and the ion solubility (sum of Si and Al, Fig. 1) after 48 h is shown for the clinker-free model systems in Fig. 9 and in Fig. 10 for the model cement systems. These correlations confirm the expected relationship between the determined DoR of the meta-phyllosilicates and their evolved heat from the reaction test as well as their Si and Al solubility. The coefficient of correlation (R^2) is higher for the model cement than for the clinker-free model system. The absence of the sulfate carrier in the clinker-free MK/MI/MS/MM-CH model systems (dashed line, Fig. 9) is a hindrance for the correlation which demonstrates the importance of the sulfate carrier for the reaction and heat release of the Al dissolved from the meta-phyllosilicates. Care must be taken when trying directly to derive of the degree of reaction of the meta-phyllosilicates from the evolved heat or Si and Al solubility, since the physical and surface properties of the meta-phyllosilicates also have a significant effect on the reaction behavior of the composite cements [9]. Nevertheless, a significant reaction contribution can be expected from CC, even from 2:1 meta-phyllosilicates, already during early hydration and thus also during the main reaction of the cement clinker phases.

A further classification of the reactivity of the calcined meta-phyllosilicates can be derived from their CH consumption (Fig. 11) and the C-S-H formation (Fig. 12). The values of MK, MI and MM in both figures are adopted from [10]. For a better clarity, Fig. 12 shows the trend lines for the C-S-H formation only from 12 h onwards. A CH consumption by MS is observable after approx. 20 h and the values range between MM (no CH consumption) and MI. The MM trend lines of C-S-H formation are also in the range of MI. Uncertainties due to the quantification with the PONKCS method and the assumption of a C-S-H composition during early hydration according to [58,59] have already been presented and discussed in connection with quantifications in systems with MK, MI and MM [10]. Analogous to the DoR, the CH consumption and C-S-H formation of the MS is in the range of the MI.

Overall, the preceding investigations of the clinker-free [8] and the model cement systems [10] reveal comparable reactivity of the 2:1 clay minerals MS and MI during early hydration. 2:1 meta-phyllosilicates

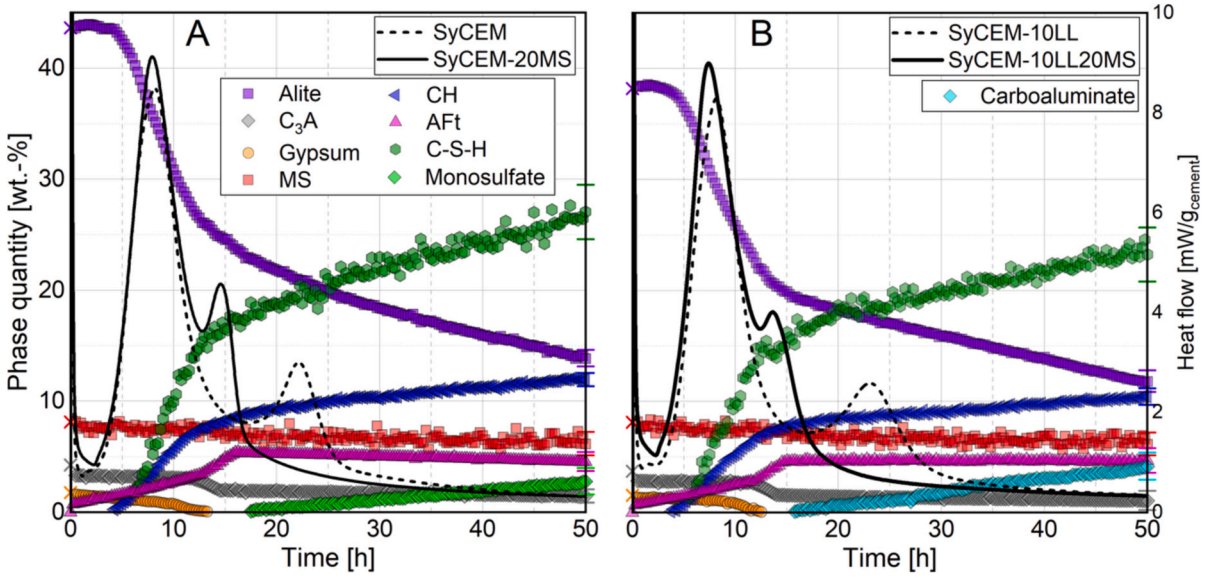

Fig. 7. Combined illustration of in situ XRD quantifications (left y-axis) and calorimeter measurements (right y-axis) of SyCEM-20MS (A) and SyCEM-10LL20MS (B). Additionally, the calorimeter curve of the reference systems taken from [10] is provided. The error bar of a duplicate determination after 50 h is shown. In the case of MS, this was used to calculate their degree of reaction.

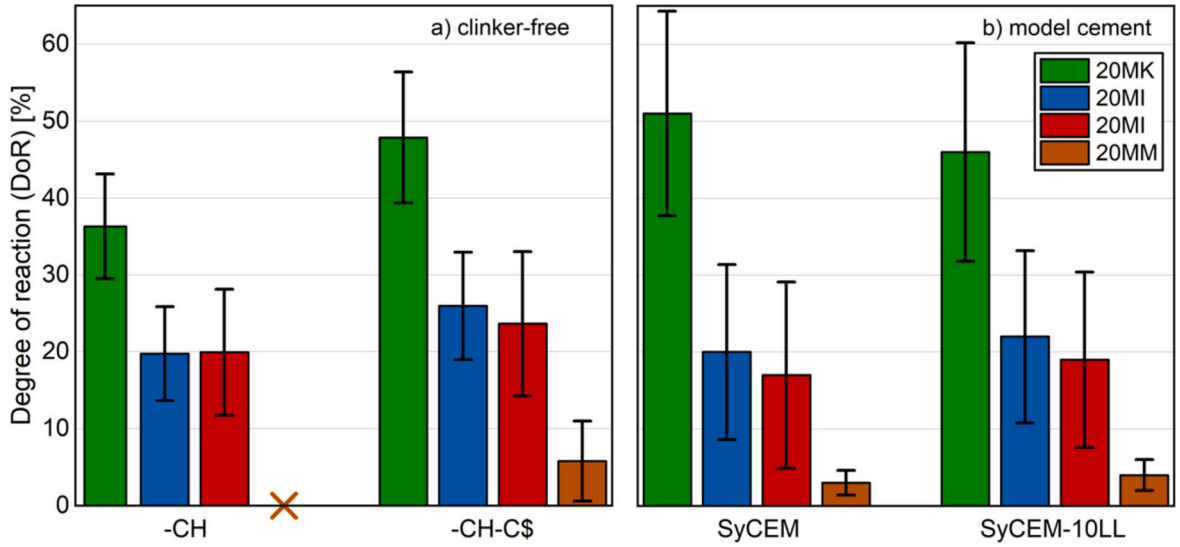

Fig. 8. DoR of the meta-phyllosilicates after 50 h in clinker-free model systems (A) and model cement systems (B). The values for MK, MI and MM for the clinker-free system are taken from [8], for the model cement systems from [10]. The error bars were determined using the values after 50 h from Figs. 5 and 7.

from the mica group (MM) exhibit no reactivity in this respect. MS can form hydrate phases solely with CH and even more in combination with CH and C$ as reaction partners. An incongruent dissolution process of MS as stated by [18] might be the driving force for a higher reactivity of the MS compared to MI from two days onwards. In both the clinker-free and the model cement systems, MS goes through a continuous dissolution process and thus exhibits clear reactivity even during early hydration.

3.4.2. Influence of meta-phyllosilicates on the clinker reaction and the sulfate balance

The influence of MS on the silicate clinker reaction is illustrated by the DoH of alite derived from XRD quantifications in Fig. 13. In comparison to the corresponding reference systems, MS induces a rather insignificant reduction of the DoH of alite. This is consistent with the already published data added in Fig. 13 from [10]. The authors assume that the aluminum in pore solution (chemical reactivity of the meta-phyllosilicates) and sulfate balance (adsorption on surfaces of the meta-phyllosilicate particles) in the pore solution are, to a certain extent, responsible for the inhibition of the alite reaction. A high amount of aluminum dissolved from the meta-phyllosilicates, therefore leads to a stronger inhibition of the silicate reaction and, thus, to a lower DoH. A difference between the MS system without (SyCEM-20MS) and with LL (SyCEM-10LL20MS) can only be observed at the beginning of alite hydration (5–20 h after water addition). After 50 h, the DoH reaches 67.9 wt-% in the SyCEM-20MS and 69.0 wt-% in the SyCEM-10LL20MS. Thus, the impact of LL appears to be lower on MS than on MK and MI.

It is much more difficult to identify the influence of the meta-phyllosilicate on the aluminate clinker reaction. Table 5 summarizes the key data regarding the aluminate reaction of the MS systems compared to the reference from [10]. As already seen from the combined representation of the heat flow and the XRD quantifications, the onset of

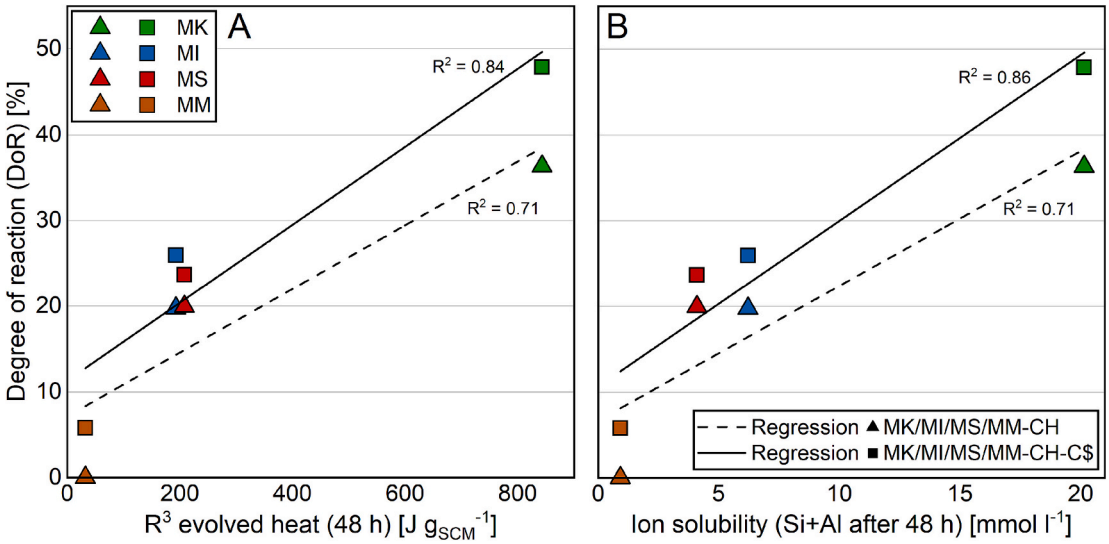

Fig. 9. Correlation of the DoR of the clinker-free model systems with the evolved heat of the reaction test (Fig. 2) after 48 h (A) and the ion solubility (sum of Si and Al, Fig. 1) after 48 h (B).

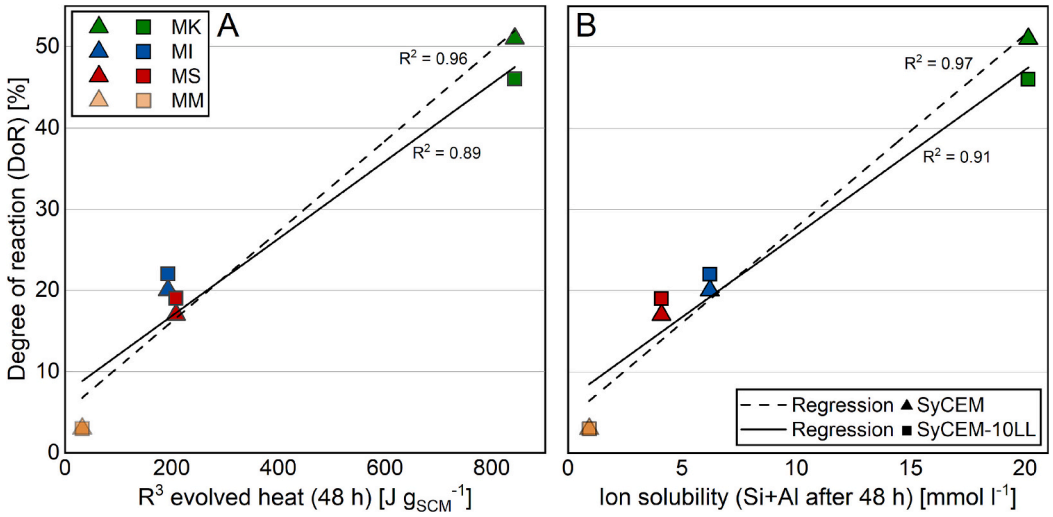

Fig. 10. Correlation of the DoR of the model cement systems with the evolved heat of the reaction test (Fig. 2) after 48 h (A) and the ion solubility (sum of Si and Al, Fig. 1) after 48 h (B).

the accelerated AFt formation with the addition of MS is around 7–8 h earlier than in the corresponding reference system. As already discussed in [10], the differences of the reaction rate is almost negligible and within the quantifiable error. Overall, the results are in line with the studies of MK, MI, and MM from [10].

The influence of the meta-phyllosilicates on the sulfate balance is presented in Fig. 14. The results of investigations with MK, MI, MM [10], and MS illustrate the difference between the pure filler effect, as in the case of MM, and the obvious influence of surface properties and chemical reactivity for MS, MK, and MI. The correlation of the DoH of the alite at the time of aluminate onset (see Table 5) and the adsorbed sulfate by available surfaces (clinker, meta-phyllosilicates, hydrate phases) proves a clear reduction of the DoH of alite and a shift to higher sulfate contents. Thus, in the case of MS, the adsorption of the sulfate cannot take place exclusively on the surfaces of the C-S-H, as described by Zunino and Scrivener [60]. Adsorption of sulfate does take place on the negatively charged surfaces of the meta-phyllosilicate surfaces (see Table 1) as described [9,10]. In terms of its influence on the sulfate balance, MS ranks close to MI, between MM and MK. The higher capacity of MS to adsorb ions from the pore solution compared to MM can be partly explained by its higher BET surface area. Nevertheless, it is noticeable that the zeta potential of MS in synthetic cement pore solution is in the range of MM (−9.5 mV) and has a lower value than MI (−28.0 mV) [10]. Here, an incongruent dissolution process of the MS possibly explains the deviating behavior of MS and MM. MM behaves inert and does not dissolve at all. It can therefore be regarded as a filler. Consequently, no change in the surfaces of the MM is expected. Incongruent dissolution of the MS, on the other hand, could cause a change in its surface properties and thus its zeta potential. There are no studies on this so far. Further investigations are necessary in order to identify the fine differences between MS and MI. It must be pointed out again that the MS content is lower compared to the other meta-phyllosilicates and that this effect could be even more pronounced with higher smectite contents in the raw clay.

4. Conclusion

The complementary investigations of the metasmectite (MS) to

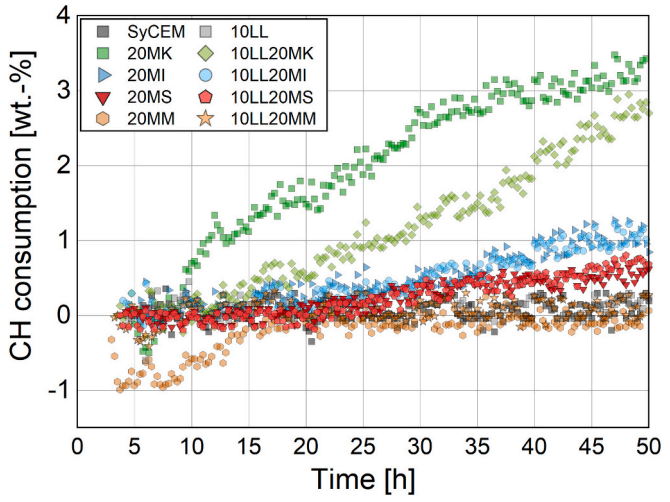

Fig. 11. CH consumption as a consequence of the pozzolanic reaction of the meta-phyllosilicates based on the calculated values from alite hydration. The reference systems, as well as the values from MK, MI, and MM, are illustrated more transparently since they are already published [10].

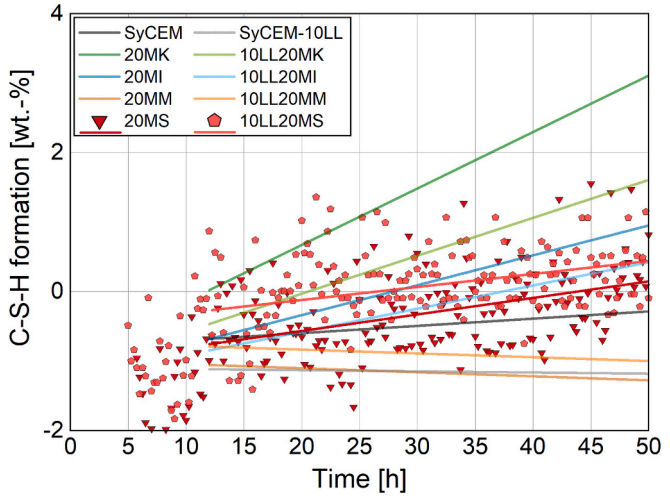

Fig. 12. C-S-H formation as a consequence of the pozzolanic reaction of the meta-phyllosilicates based on the calculated values from alite hydration. The individual values of the reference systems, as well as MK, MI, and MM, are not shown for a better overview, but only the trend lines from 12 h onwards.

investigations of metakaolinite (MK), metaillite (MI) and meta-muscovite (MM) [8,10] in clinker-free model and in model cement systems lead to the following conclusions:

- Overall, MS exhibits a proper reactivity after 7 d, while the impact on early clinker hydration is moderate.
- MS yields an autonomous hydrate phase formation in clinker-free model systems characterized by a continuous dissolution of MS and precipitation of C-S-H and AFt without a pronounced heat flow maximum after the initial heat flow.
- The silicon and aluminum solubility as well as the evolved heat from the reaction test indicate clearer differences between MS and MI from two days onwards. An incongruent dissolution of MS might explain their fine differences.
- The reactivity of the MS in cementitious systems is comparable the reactivity of MI during early hydration regarding their degree of reactivity, the CH consumption and C-S-H formation.

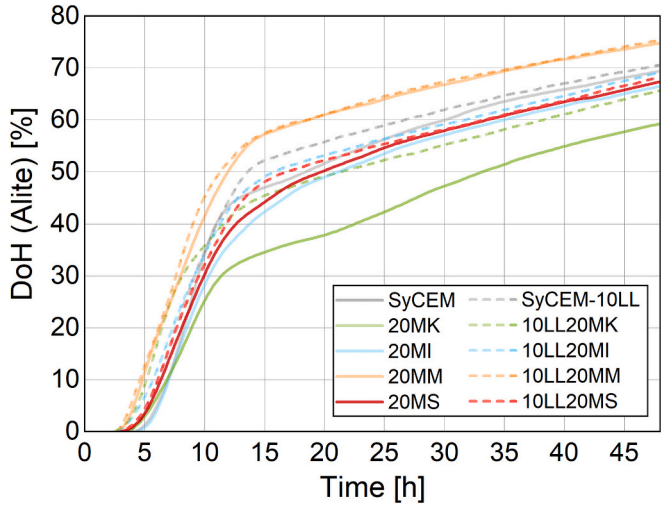

Fig. 13. Degree of Hydration (DoH) of alite calculated from XRD quantifications. The values except of MS are taken from [10].

Table 5
Summary of key data concerning the aluminate reaction.

	SyCEM	20MS	SyCEM-10LL	10LL20MS
Time onset AFt [h]	19.75	12.50	19.50	11.50
AFt Start [wt-%]	1.68	0.73	1.34	0.69
AFt at onset [wt-%]	5.77	3.60	5.06	3.09
Reaction rate [wt-%/h]	0.21	0.23	0.19	0.21
[1]Monosulfate/[2]Hemicarboaluminate [wt-%]	1.9[1]	2.8[1]	3.7[2]	4.2[2]

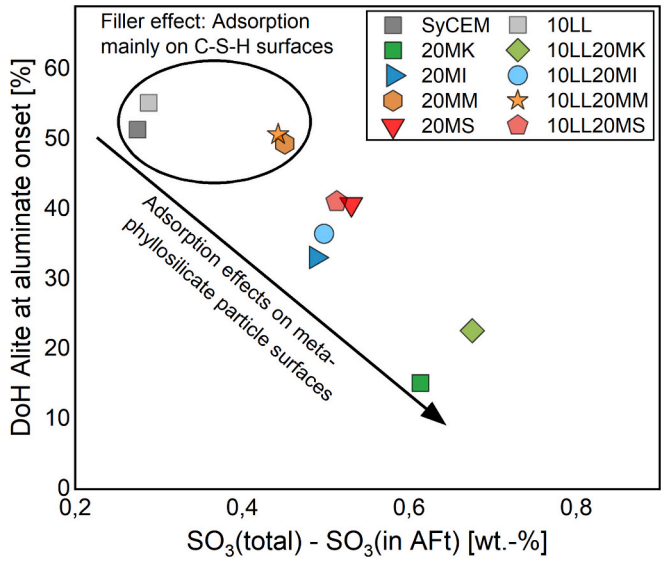

Fig. 14. Correlation of the SO_3 content with the DoH of alite at the onset of accelerated AFt formation. The SO_3 content is calculated as difference between the total SO_3 content and the SO_3 bound in AFt analogous to [9]. The MS values are supplemented with data from [10].

- The addition of MS accelerates the aluminate clinker reaction and impedes the alite reaction rather insignificant and to a much lower extend than MK.
- MS affect the sulfate balance of the cementitious system by adsorbing ions from the pore solution on its negatively charged surfaces

CRediT authorship contribution statement

Sebastian Scherb: Writing – original draft, Validation, Methodology, Investigation, Data curation, Conceptualization. **Matthias Maier:** Validation, Data curation. **Nancy Beuntner:** Writing – review & editing, Project administration, Funding acquisition, Conceptualization. **Karl-Christian Thienel:** Writing – review & editing.

Declaration of competing interest

The authors declare that they have no known competing financial interests or personal relationships that could have appeared to influence the work reported in this paper.

Acknowledgement

The authors like to thank Deutsche Forschungsgemeinschaft (DFG) for the financial support of the research project "Efficiency and influence of calcined phyllosilicates during the early hydration of cement" (438621761). The work of M. Maier was supported by the Fraunhofer Internal Programs under Grant No. Attract 40-06135.

Appendix A

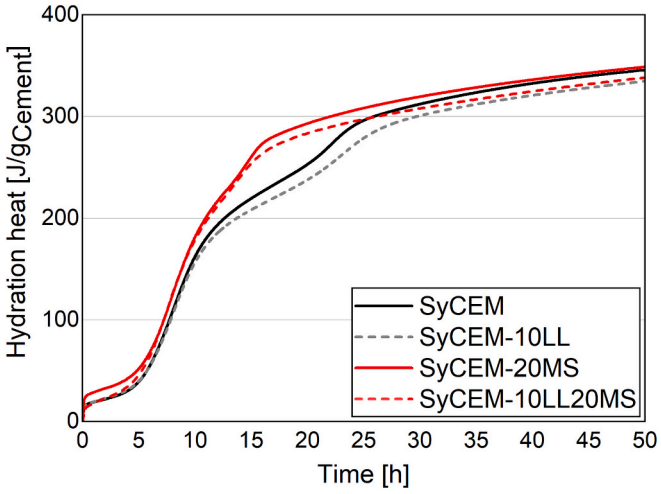

Fig. 15. Hydration heat of the SyCEM and SyCEM-MS systems calculated from the heat flow of Fig. 7.

Data availability

Data will be made available on request.

References

[1] K.L. Scrivener, V.M. John, E.M. Gartner, in: United Nations Environment Programme (Ed.), Eco-efficient Cements: Potential, Economically Viable Solutions for a Low-CO_2, Cement-based Materials Industry, United Nations Environment Programme, Paris, France, 2016, p. X, 50.

[2] R. Sposito, M. Maier, G. Cordoba, S. Scherb, A. Tironi, N. Beuntner, A. Neißer-Deiters, E.F. Irassar, K.-C. Thienel, Transferability from pure metaphases to calcined common clays – new insights into particle properties and prediction models, in: M. Sharma, H. Hafez, F. Zunino, K. Scrivener (Eds.), International Conference on Calcined Clays for Sustainable ConcreteLausanne, Switzerland, 2022, pp. 110–111.

[3] M. Maier, N. Beuntner, K.-C. Thienel, An approach for the evaluation of local raw material potential for calcined clay as SCM, based on geological and mineralogical data: examples from German clay deposits, in: S. Bishnoi (Ed.), Calcined Clays for Sustainable Concrete - Proceedings of the 3rd International Conference on Calcined Clays for Sustainable Concrete, Springer, Singapore, 2020, pp. 37–47, https://doi.org/10.1007/978-981-15-2806-4_5.

[4] R.J. Myers, G. Geng, J. Li, E.D. Rodríguez, J. Ha, P. Kidkhunthod, G. Sposito, L. N. Lammers, A.P. Kirchheim, P.J.M. Monteiro, Role of adsorption phenomena in cubic tricalcium aluminate dissolution, Langmuir 33 (2017) 45–55, https://doi.org/10.1021/acs.langmuir.6b03474.

[5] E.M.J. Bérodier, A.C.A. Muller, K.L. Scrivener, Effect of sulfate on C-S-H at early age, Cem. Concr. Res. 138 (2020) 106248, https://doi.org/10.1016/j.cemconres.2020.106248.

[6] F. Zunino, K. Scrivener, Factors influencing the sulfate balance in pure phase C_3S/C_3A systems, Cem. Concr. Res. 133 (2020) 106085, https://doi.org/10.1016/j.cemconres.2020.106085.

[7] M. Maier, S. Scherb, A. Neißer-Deiters, N. Beuntner, K.-C. Thienel, Hydration of cubic tricalcium aluminate in the presence of calcined clays, J. Am. Ceram. Soc. 104 (2021) 3619–3631, https://doi.org/10.1111/jace.17745.

[8] S. Scherb, M. Maier, N. Beuntner, K.-C. Thienel, J. Neubauer, Reaction kinetics during early hydration of calcined phyllosilicates in clinker-free model systems, Cem. Concr. Res. 143 (2021) 106382, https://doi.org/10.1016/j.cemconres.2021.106382.

[9] M. Maier, R. Sposito, N. Beuntner, K.-C. Thienel, Particle characteristics of calcined clays and limestone and their impact on the early hydration and sulfate demand of blended cement, Cem. Concr. Res. 154 (2022) 15, https://doi.org/10.1016/j.cemconres.2022.106736.

[10] S. Scherb, M. Maier, M. Köberl, N. Beuntner, K.-C. Thienel, Reaction kinetics during early hydration of calcined phyllosilicates in model cement systems, Cem. Concr. Res. 175 (2024) 107356, https://doi.org/10.1016/j.cemconres.2023.107356.

[11] M. Maier, S. Scherb, K.-C. Thienel, Sulfate consumption during the hydration of Alite and its influence by SCMs, Vortrag auf der 21, in: Internationale Baustofftagung ibausil, 13.-15. September 2023 in Weimar, 2023.

[12] A. Quennoz, K.L. Scrivener, Interactions between alite and C_3A-gypsum hydrations in model cements, Cem. Concr. Res. 44 (2013) 46–54, https://doi.org/10.1016/j.cemconres.2012.10.018.

[13] L. Valentini, M. Dalconi, M. Favero, G. Artioli, G. Ferrari, In-situ XRD measurement and quantitative analysis of hydrating cement: implications for sulfate incorporation in C–S–H, J. Am. Ceram. Soc. 98 (2015) 1259–1264, https://doi.org/10.1111/jace.13401.

[14] C. He, E. Makovicky, B. Osbæck, Thermal stability and pozzolanic activity of raw and calcined mixed-layer mica/smectite, Appl. Clay Sci. 17 (2000) 141–161, https://doi.org/10.1016/S0169-1317(00)00011-9.

[15] R. Fernandez, F. Martirena, K.L. Scrivener, The origin of the pozzolanic activity of calcined clay minerals: a comparison between kaolinite, illite and montmorillonite, Cem. Concr. Res. 41 (2011) 113–122, https://doi.org/10.1016/j.cemconres.2010.09.013.

[16] S. Hollanders, R. Adriaens, J. Skibsted, Ö. Cizer, J. Elsen, Pozzolanic reactivity of pure calcined clays, Appl. Clay Sci. 132–133 (2016) 552–560, https://doi.org/10.1016/j.clay.2016.08.003.

[17] T. Danner, G. Norden, H. Justnes, Calcareous smectite clay as a pozzolanic alternative to kaolin, Eur. J. Environ. Civ. Eng. (2019) 1–18, https://doi.org/10.1080/19648189.2019.1590741.

[18] N. Garg, J. Skibsted, Dissolution kinetics of calcined kaolinite and montmorillonite in alkaline conditions: evidence for reactive Al(V) sites, J. Am. Ceram. Soc. 102 (2019) 7720–7734, https://doi.org/10.1111/jace.16663.

[19] N. Werling, J. Kaltenbach, P.G. Weidler, R. Schuhmann, F. Dehn, K. Emmerich, Solubility of calcined kaolinite, montmorillonite, and illite in high molar NaOH and suitability as precursors for geopolymers, Clay Clay Miner. 70 (2022), https://doi.org/10.1007/s42860-022-00185-6.

[20] C. He, E. Makovicky, B. Osbæck, Thermal stability and pozzolanic activity of calcined illite, Appl. Clay Sci. 9 (1995) 337–354, https://doi.org/10.1016/0169-1317(94)00033-M.

[21] S. Scherb, N. Beuntner, K.-C. Thienel, Reaction kinetics of the basic clays present in natural mixed clays, in: F. Martirena, A. Favier, K. Scrivener (Eds.), Proceedings of the 2nd International Conference on Calcined Clays for Sustainable Concrete, Springer, Dordrecht, Netherlands, 2018, pp. 427–433, https://doi.org/10.1007/978-94-024-1207-9_69.

[22] R. Sposito, M. Maier, N. Beuntner, K.-C. Thienel, Evaluation of zeta potential of calcined clays and time-dependent flowability of blended cement with customized polycarboxylate-based superplasticizers, Constr. Build. Mater. 308 (2021) 125061, https://doi.org/10.1016/j.conbuildmat.2021.125061.

[23] DIN ISO 9277, Determination of the Specific Surface Area of Solids by Gas Adsorption - BET Method, Beuth-Verlag, Berlin, Germany, 2003, p. 19.

[24] DIN EN ISO 17892-3, Geotechnical Investigation and Testing - Laboratory Testing of Soil - Part 3: Determination of Particle Density, Beuth-Verlag, Berlin, Germany, 2015, p. 21.

[25] S. Scherb, N. Beuntner, K.-C. Thienel, J. Neubauer, Quantitative X-ray diffraction of free, not chemically bound water with the PONKCS method, J. Appl. Crystallogr. 51 (2018) 1535–1543, https://doi.org/10.1107/S1600576718012888.

[26] A. Buchwald, R. Kriegel, C. Kaps, H.-D. Zellmann, Untersuchung zur Reaktivität von Metakaolinen für die Verwendung in Bindemittelsystemen, Gesellschaft Deutscher Chemiker e.V. - Jahrestagung, Gesellschaft Deutscher Chemiker e.V., Frankfurt, Germany, 2003, pp. 91–97.

[27] ASTM C1897 - 20, Standard Test Methods for Measuring the Reactivity of Supplementary Cementitious Materials by Isothermal Calorimetry and Bound Water Measurements, ASTM International, West Conshohocken, PA, 2020, p. 10, https://doi.org/10.1520/C1897-20.

[28] H.M. Rietveld, Line profiles of neutron powder-diffraction peaks for structure refinement, Acta Crystallogr. 22 (1967) 151–152, https://doi.org/10.1107/S0365110X67000234.

[29] H.M. Rietveld, An Algol Program for the Refinement of Nuclear and Magnetic Structures by the Profile Method, RCN, Reactor Centrum Nederland, 1969.

[30] D. Jansen, F. Goetz-Neunhoeffer, C. Stabler, J. Neubauer, A remastered external standard method applied to the quantification of early OPC hydration, Cem. Concr. Res. 41 (2011) 602–608, https://doi.org/10.1016/j.cemconres.2011.03.004.

[31] N.V.Y. Scarlett, I.C. Madsen, Quantification of phases with partial or no known crystal structures, Powder Diffract. 21 (2006) 278–284, https://doi.org/10.1154/1.2362855.

[32] S.T. Bergold, F. Goetz-Neunhoeffer, J. Neubauer, Quantitative analysis of C–S–H in hydrating alite pastes by in-situ XRD, Cem. Concr. Res. 53 (2013) 119–126, https://doi.org/10.1016/j.cemconres.2013.06.001.

[33] T. Degen, M. Sadki, E. Bron, U. König, G. Nénert, The HighScore suite, Powder Diffract. 29 (2014) S13–S18, https://doi.org/10.1017/S0885715614000840.

[34] M.C. Neuburger, Präzisionsmessung der Gitterkonstante von Silicium, Z. Kristallogr. Cryst. Mater. (1935) 313, https://doi.org/10.1524/zkri.1935.92.1.313.

[35] Á.G. De La Torre, S. Bruque, J. Campo, M.A.G. Aranda, The superstructure of C3S from synchrotron and neutron powder diffraction and its role in quantitative phase analyses, Cem. Concr. Res. 32 (2002) 1347–1356, https://doi.org/10.1016/S0008-8846(02)00796-2.

[36] P. Mondal, J.W. Jeffery, The crystal structure of tricalcium aluminate, $Ca_3Al_2O_6$, Acta Crystallogr. B 31 (1975) 689–697, https://doi.org/10.1107/S0567740875003639.

[37] P.F. Schofield, C.C. Wilson, K.S. Knight, I.C. Stretton, Temperature related structural variation of the hydrous components in gypsum, Z. Kristallogr. Cryst. Mater. 215 (2000) 707, https://doi.org/10.1524/zkri.2000.215.12.707.

[38] A. Kirfel, G. Will, Charge density in anhydrite, CaSO4, from X-ray and neutron diffraction measurements, Acta Crystallogr. B 36 (1980) 2881–2890, https://doi.org/10.1107/S0567740880010461.

[39] A. Viani, A. Gualtieri, G. Artioli, The nature of disorder in montmorillonite by simulation of X-ray powder patterns, Am. Mineral. 87 (2002), https://doi.org/10.2138/am-2002-0720.

[40] V.A. Drits, B.B. Zviagina, D.K. McCarty, A.L. Salyn, Factors responsible for crystal-chemical variations in the solid solutions from illite to aluminoceladonite and from glauconite to celadonite, Am. Mineral. 95 (2010) 348–361, https://doi.org/10.2138/am.2010.3300.

[41] M. Catti, G. Ferraris, G. Ivaldi, Thermal strain analysis in the crystal structure of muscovite at 700 °C, Eur. J. Mineral. 1 (1989) 625–632, https://doi.org/10.1127/ejm/1/5/0625.

[42] Y. Le Page, G. Donnay, Refinement of the crystal structure of low-quartz, Acta Crystallogr. Sect. B: Struct. Sci. 32 (1976) 2456–2459, https://doi.org/10.1107/S0567740876007966.

[43] M. Horn, C.F. Schwerdtfeger, E.P. Meagher, Refinement of the structure of anatase at several temperatures, Z. Kristallogr. Cryst. Mater. 136 (1972) 273–281, https://doi.org/10.1524/zkri.1972.136.3-4.273.

[44] F.F. Foit Jr., D.R. Peacor, The anorthite crystal structure at 410 and 830°C, Am. Mineral. 58 (1973) 665–675.

[45] W.R. Busing, H.A. Levy, Neutron diffraction study of calcium hydroxide, J. Chem. Phys. 26 (1957) 563–568, https://doi.org/10.1063/1.1743345.

[46] F. Goetz-Neunhoeffer, J. Neubauer, Refined ettringite ($Ca_6Al_2(SO_4)_3(OH)_{12}\bullet 26H_2O$) structure for quantitative X-ray diffraction analysis, Powder Diffract. 21 (2005) 4–11, https://doi.org/10.1154/1.2146207.

[47] T. Runcevski, R.E. Dinnebier, O.V. Magdysyuk, H. Pöllmann, Crystal structures of calcium hemicarboaluminate and carbonated calcium hemicarboaluminate from synchrotron powder diffraction data, Acta Crystallogr. B 68 (2012) 493–500, https://doi.org/10.1107/S010876811203042X.

[48] C. Hoffmann, T. Armbruster, Clinotobermorite, Ca5[Si3O8(OH)]2 · 4 H2O - Ca5[Si6O17] · 5 H2O, a natural C-S-H(I) type cement mineral: determination of the substructure, Z. Kristallogr. Cryst. Mater. (1997) 864, https://doi.org/10.1524/zkri.1997.212.12.864.

[49] R. Allmann, Refinement of the hybrid layer structure $[Ca_2Al(OH)_6]^+$ $[1/2SO_4\ 3H_2O]^-$, Neues Jahrb. Mineral. 3 (1977) 136–144.

[50] H. Pöllmann, J. Kuzel H., PDF Data Sheet: 42-0062, Calcium Aluminum Sulfate Hydrate, Mineralogical Institute of University Erlangen, ICDD Grant-in-Aid, 1990.

[51] C. Hesse, F. Goetz-Neunhoeffer, J. Neubauer, A new approach in quantitative in-situ XRD of cement pastes: correlation of heat flow curves with early hydration reactions, Cem. Concr. Res. 41 (2011) 123–128, https://doi.org/10.1016/j.cemconres.2010.09.014.

[52] T. Matschei, B. Lothenbach, F.P. Glasser, The role of calcium carbonate in cement hydration, Cem. Concr. Res. 37 (2007) 551–558, https://doi.org/10.1016/j.cemconres.2006.10.013.

[53] B. Lothenbach, M. Zajac, Application of thermodynamic modelling to hydrated cements, Cem. Concr. Res. 123 (2019) 105779, https://doi.org/10.1016/j.cemconres.2019.105779.

[54] S. Scherb, M. Köberl, N. Beuntner, K.-C. Thienel, J. Neubauer, Reactivity of metakaolin in alkaline environment: correlation of results from dissolution experiments with XRD quantifications, Materials 13 (2020) 18, https://doi.org/10.3390/ma13102214.

[55] F. Avet, X. Li, K. Scrivener, Determination of the amount of reacted metakaolin in calcined clay blends, Cem. Concr. Res. 106 (2018) 40–48, https://doi.org/10.1016/j.cemconres.2018.01.009.

[56] F. Avet, X. Li, K. Scrivener, Methods to determine the reaction degree of metakaolin in cementitious blends, in: J. Gemrich (Ed.), 15th International Congress on the Chemistry of Cement, Prague, Czech Republic, Research Institute of Binding Materials Prague, 2019, p. 6.

[57] R. Snellings, P. Suraneni, J. Skibsted, Future and emerging supplementary cementitious materials, Cem. Concr. Res. 171 (2023) 107199, https://doi.org/10.1016/j.cemconres.2023.107199.

[58] A.T. Allen, J. J., H.M. Jennings, Composition and density of nanoscale calcium-silcate-hydrate in cement, Nat. Mater. 6 (4) (2007) 311–316, https://doi.org/10.1038/nmat1871.

[59] I.G. Richardson, The nature of C-S-H in hardened cements, Cem. Concr. Res. 29 (1999) 1131–1147, https://doi.org/10.1016/S0008-8846(99)00168-4.

[60] F. Zunino, K. Scrivener, Insights on the role of alumina content and the filler effect on the sulfate requirement of PC and blended cements, Cem. Concr. Res. 160 (2022) 106929, https://doi.org/10.1016/j.cemconres.2022.106929.